Original Article

Isolation of SARS-CoV-2 B.1.1.28.2 (P2) variant and pathogenicity comparison with D614G variant in hamster model

Pragya Yadav [a],[*], Sreelekshmy Mohandas [a], Prasad Sarkale [a], Dimpal Nyayanit [a], Anita Shete [a], Rima Sahay [a], Varsha Potdar [a], Shrikant Baradkar [a], Nivedita Gupta [b], Gajanan Sapkal [a], Priya Abraham [a], Samiran Panda [b], Balram Bhargava [b]

[a] Indian Council of Medical Research-National Institute of Virology (ICMR-NIV), Pune, Maharashtra, 411021, India
[b] Indian Council of Medical Research, V. Ramalingaswami Bhawan, P.O. Box No. 4911, Ansari Nagar, New Delhi, 110029, India

ARTICLE INFO

ABSTRACT

Background: Considering the potential threat from emerging Severe Acute Respiratory Syndrome-Corona Virus-2 (SARS-CoV-2) variants and the rising COVID-19 cases, SARS-CoV-2 genomic surveillance is ongoing in India. We report herewith the isolation of the P.2 variant (B.1.1.28.2) from international travelers and further its pathogenicity evaluation and comparison with D614G variant (B.1) in hamster model.
Methods: Virus isolation was performed in Vero CCL81 cells and genomic characterization by next generation sequencing. The pathogenicity and host immune response of the isolate was assessed in Syrian hamster model and compared with B.1 variant.
Results: B.1.1.28.2 variant was isolated from nasal/throat swabs of international travelers returned to India from United Kingdom and Brazil. The B.1.1.28.2 variant induced body weight loss, viral replication in the respiratory tract and caused severe lung pathology in infected Syrian hamster model in comparison, with B.1 variant infected hamsters. The sera from B.1.1.28.2 infected hamsters efficiently neutralized the D614G variant virus whereas 6-fold reduction in the neutralization was seen in case of D614G variant infected hamsters' sera with the B.1.1.28.2 variant.
Conclusions: B.1.1.28.2 lineage variant could be successfully isolated and characterization could be performed. Pathogenicity of the isolate was demonstrated in Syrian hamster model and the findings of neutralization reduction is of great concern and point towards the need for screening the vaccines for efficacy.

Introduction

Over the year of COVID-19 pandemic, Severe Acute Respiratory Syndrome Corona virus-2 (SARS-CoV-2) has accumulated several mutations leading to the emergence of new variants. The first SARS-CoV-2 variant of concern (VOC), B.1.1.7 (also known as Alpha variant) was identified in late December in the United Kingdom (UK) which is now reported in more than 195 countries worldwide as on 3rd October 2021. This variant has about 17 mutations, including N501Y, P681H, 69–70 deletion; the ORF8 Q27stop mutation outside the spike protein and is adapted to be more transmissible. Subsequently, another variant B.1.351 (Beta variant) was identified in South Africa with 21 mutations, including N501Y, E484K, and

K417N on the spike protein, and ORF1b deletion outside the spike protein. It has been reported in Africa, Europe, Asia, and Australia with studies reporting potential immune escape [2].

During January 2021, lineage P.1, also known as Gamma variant, a VOC with 17 amino acid changes which includes N501Y, E484K, and K417N on the spike protein; ORF1b deletion outside the spike protein was detected in the travelers from Brazil at Japan. The virus has been found to be widely distributed in Amazonas state of Brazil and also noticed in the Faroe Islands, South Korea, and USA [3,4]. The virulence, transmissibility and immune invasion potential of this variant remains unknown. Still, there is a concern that this variant might have facilitated the re-infections in Manus city of Amazonas which had achieved herd immunity in October 2020. Furthermore, Brazil reported another variant P.2 lineage, which has E484K mutation but not the N501Y and K417N amino acid changes in the spike protein [3]. On 11th May 2021, B.1.617.2 was designated as VOC by World Health Organisation

which has shown higher transmission potential than any of the SARS-CoV-2 variants reported till date [5,6]. Other than the 4 listed VOCs, many SARS-CoV-2 variants were designated as Variants of Interest (VOI) like B.1.525 (Eta), B.1.526 (Iota), B.1.617.1 (Kappa), C.37 (Lambda), B.1.429/B.1.427 (Epsilon), P.2 (Zeta), P.3 (Theta), B.1.621 (Mu) [6]. The mutations in receptor binding domain (RBD) of the spike protein enabled these variants to have strong affinity and binding capacity to receptor Angiotensin converting enzyme 2 (ACE2) leading to higher transmissibility [1–4]. Also, many of these variants are reported to be linked to the immune escape and neutralization reduction threatening the vaccine policies and potential monoclonal antibody treatments [7,8].

Pathogenicity of the SARS-CoV-2 virus variants can be assessed in animal models. For SARS CoV-2 multiple animal models are available like ferrets, Syrian hamsters, non-human primates etc [9]. Among this, Syrian hamster is a widely used model for SARS-CoV-2 which develops pneumonia and body weight loss following infection [10]. Syrian hamsters have been used to assess the pathogenicity of many SARS-CoV-2 variants like B.1, B.1.1.7, B.1.617 [10,11].

Considering the potential threat from emerging variants, the Government of India has continued the SARS-CoV-2 genomic surveillance of the International travelers and their contact tracing. Here, we report isolation and characterization of the P.2/Zeta (B.1.1.28.2) variant from clinical specimens of international travelers and its pathogenesis in Syrian hamsters in comparison with B.1 variant, an early virus isolate with D614G mutation.

Methods

Clinical specimens

The throat/nasal swabs of international travelers, who returned from UK and Brazil during the month of December, 2020 and January, 2020 were collected for COVID-19 screening. SARS-CoV-2 real time RT-PCR positive samples were sequenced by NGS and virus isolation was attempted. These samples were chosen for isolation considering the quality of sample, transport storage conditions, cycle threshold value in realtime RT-PCR and the genome sequence. Two COVID-19 asymptomatic cases (aged 69 and 26 years) of international travelers who returned from UK (in December 2020) and Brazil (in January 2021) respectively to India were found positive for SARS-CoV-2 belonging to the B.1.1.28.2 lineage. Both the cases did not have any co-morbid conditions and were asymptomatic throughout the course of infection till recovery.

Virus isolation and titration

Vero CCL81 cells grown in Minimum Essential Media (MEM) supplemented with 2% fetal bovine serum (FBS) were used. Hundred microliters of the tissue homogenate/swab specimens were added onto a 24-well plate of VeroCCL81 cells and incubated at 37 °C for one hour. After washing with phosphate buffered saline and removal of media, the plates were incubated with maintenance media in a CO_2 incubator at 37 °C. The plates were observed daily for any cytopathic effects (CPE) using an inverted microscope (Nikon, Eclipse Ti, Japan). On observation of CPE, the supernatant was harvested and confirmed by real-time RT-PCR. Titration was performed by Reed and Muench method and titer was expressed as TCID50/mL [12].

SARS-CoV-2 B.1 variant (D614G variant), NIV-2020-770 (GISAID identifier: EPI_ISL_420546) isolated from a patient's throat/nasal swab sample with a titre of $10^{6.5}$ tissue culture infective dose 50 (TCID50)/mL was used for the pathogenicity comparison

study in hamsters with the B.1.1.28.2 isolate (GISAID identifier: EPI_ISL_2013029) [13].

Next generation sequencing

Genomic characterization of clinical samples and virus isolates were carried out using Next-Generation Sequencing (NGS) as per earlier explained protocols [14]. Briefly, swabs and tissue culture fluid (TCF) of viral isolates were processed for RNA extraction using Magmax RNA extraction kit (Applied Biosystems, USA) as per the manufacturer's instructions. The total RNA was extracted from 200−400 μl of the SARS-CoV-2 real-time RT-PCR positive clinical samples/ TCF. RNA was eluted into a 50 μL of elution buffer. Quantification of the extracted RNA was performed with the Qubit RNA High Sensitivity kit using a Qubit 2.0 Fluorometer (Invitrogen, Carlsbad, CA, USA). For the NGS, ribosomal RNA depletion was carried on the extracted RNA using Nebnext rRNA depletion kit (Human/mouse/rat) (New England BioLabs. In, USA). Subsequently, cDNA was synthesized with the first strand and second strand synthesis kit. The RNA libraries were prepared using TruSeq Stranded total RNA library preparation kit (Illumina, USA). The amplified RNA libraries were quantified using KAPA Library Quantification Kit (Kapa Biosystems; Roche Diagnostics Corporation, Indianapolis, IN, USA). Quantified libraries were diluted and loaded after normalization on the MiSeq Illumina sequencing platform described earlier [6]. The genomic sequences for the clinical specimens and the virus isolates were retrieved using the reference-based mapping with the SARS-CoV-2 reference sequence (Accession Number: NC_045512.2) in CLC Genomics Workbench v20.0.4 and submitted to the public repository i.e., GISAID. The retrieved sequences were aligned with other representative SARSCoV-2 sequences downloaded from the GISAID database and a phylogenetic tree was generated with representative sequences from GISAID. General Time Reversible model with Gamma distribution of 0.05 and a bootstrap replication of 1000 cycles was used to generate a Maximum-Likelihood tree.

Ethics statement

The ethical approvals were received from Institutional Ethics committee, ICMR-National Institute of Virology for the study involving human samples (Approval no: NIV/IEC/Jan/2020/ D-10). All the animal experiments were performed with the approval of Institutional Animal Ethics Committee (Approval no: NIV/IAEC/2021/ MCL/01) and as per the guidelines of Committee for the Purpose of Control and Supervision of Experiments on Animals, India.

Pathogenicity study in Syrian hamsters

To understand the pathogenicity of the isolate, we intranasally inoculated 10^4 TCID50 virus dose of P.2 (B.1.1.28.2) in 9 Syrian hamsters and observed them for 7 days for any disease and three hamsters from each group were sacrificed on day 3, 5 and 7 to study the organ viral load, antibody response and lung pathology. Simultaneously the pathogenicity of this variant was compared with a widely circulating characterized B.1 lineage SARS-CoV-2 variant in Syrian hamsters. For this, 9 hamsters were intranasally infected with 10^4 TCID50 virus dose of B.1 lineage variant and observed for any clinical signs and studied the organ viral load, antibody response and lung pathology in sacrificed animals as defined for B.1.1.28.2.

SARS-CoV-2 E gene real time RT-PCR to detect gRNA and sgRNA

Nasal wash, throat swab and organ tissue samples were collected from hamsters at necropsy. Organ samples were homog-
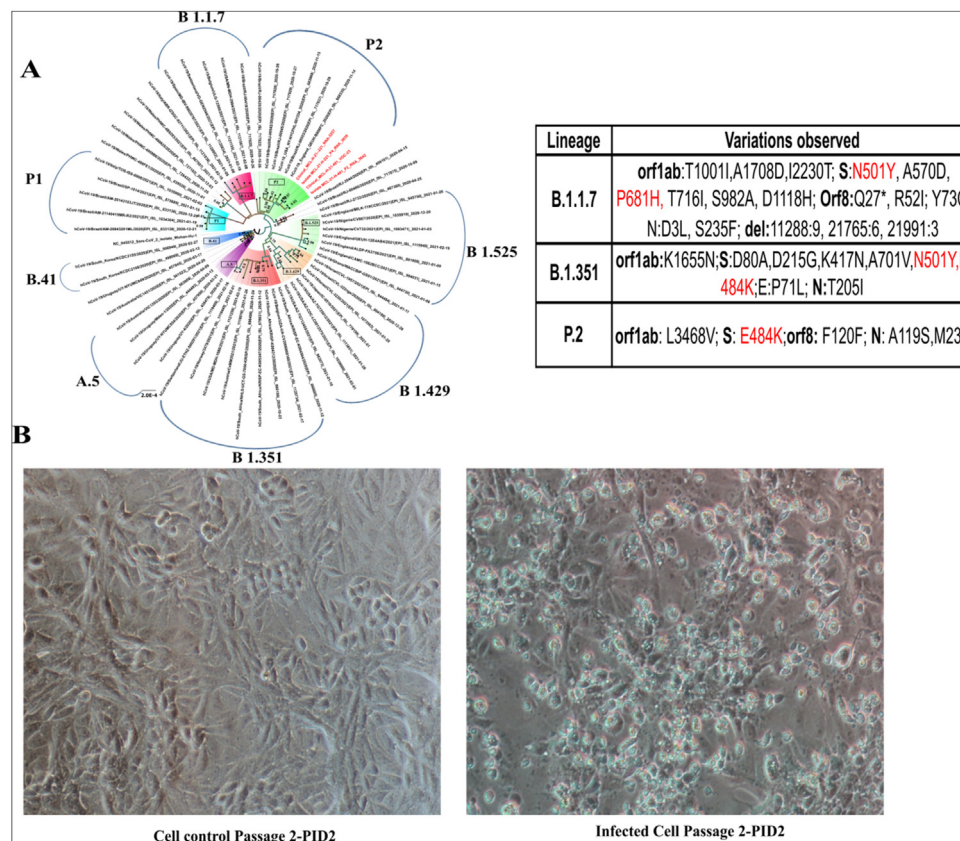
Fig. 1. Isolation and characterization of B.1.128 P2 Brazil variants: (A) Maximum likelihood tree of the clinical samples and its isolate from the international travelers. The tree was generated using general time reversible model with a bootstrap replication of 1000 cycles. The sequences retrieved in from clinical specimens and its isolates are highlighted in red (B) The cytopathic effect observed in the Vero CCL-81 cell culture at passage-2 PID-4 compared to the cell control.

enized in 1 ml cell culture media using tissue homogenizer (Eppendorf, Germany). MagMAX^{TM} Viral/Pathogen Nucleic Acid Isolation Kit was used for RNA extraction as per the manufacturer's instructions. Real-time RT-PCR was performed for SARS-CoV-2 E gene (both genomic and subgenomic RNA) as described earlier [15,16].

Enzyme-linked immunosorbent assay

The hamster serum samples collected on day 3, 5, 7 post virus inoculation were tested for IgG antibodies by hamster anti-SARS-CoV-2 IgG ELISA as described earlier [17].

Plaque reduction neutralization test (PRNT50)

PRNT50 was performed on serum samples of hamsters against SARS-CoV-2 B.1 variant and B.1.1.28.2 variant as per earlier described methodology [18].

Histopathology

For histopathological evaluation of lung lesions, lungs collected during necropsy were fixed in 10% neutral buffered formalin. The fixed lung tissues were processed using an automated tissue processor and were embedded in paraffin. The tissues were sectioned using an automated microtome (Leica, Germany) and stained by routine hematoxylin and eosin staining. The lesions were graded as severe (+4), moderately severe (+3), minimal (+2), mild (+1) and no lesions (0) after scoring for the vascular changes, alveolar damage and inflammatory changes.

Data analysis

Graph pad Prism version 8.4.3 software was used for the analysis. Non parametric Mann Whitney tests were used and the p-values less than 0.05 were considered to be statistically significant.

Results

B.1.1.28.2 isolation and characterization

Clinical specimens inoculated in to Vero CCL-81 cells showed a typical rounding and detachment of the infected cells on 4th post-inoculation day (PID) (Fig. 1). The progressive infectivity was observed with fusion of the infected cells with neighboring cells leading to the generation of large mass of cells. The presence of the replication competent virus was confirmed by Real time RT-PCR that demonstrated higher viral load in the cell culture medium on PID-3 than inoculated specimens. The virus isolate titrated at passage 2 and passage 3 demonstrated a virus titer of $10^{4.5}$ and $10^{5.13}$ TCID50/mL respectively. On phylogenetic analysis, the clinical specimens and virus isolates were found to cluster with the Brazil P2 lineage sequences. The clinical and the isolate sequences (GISAID identifier: EPI_ISL_2013029, EPI_ISL_2013033) had amino acid mutations similar to the ones reported in the Brazilian P2 variant (Fig. 1). The amino acid substitutions detected in both the isolates were D614G, E484K, V1176F in the spike, A119S, G204R, M234I, R203K in the N, L205V in NSP5, L71F in NSP7 and P32L in NSP 12. EPI_ISL_2013029 isolate showed additional substitutions N Q9H, NS3 G44V and NSP 15 K12N.
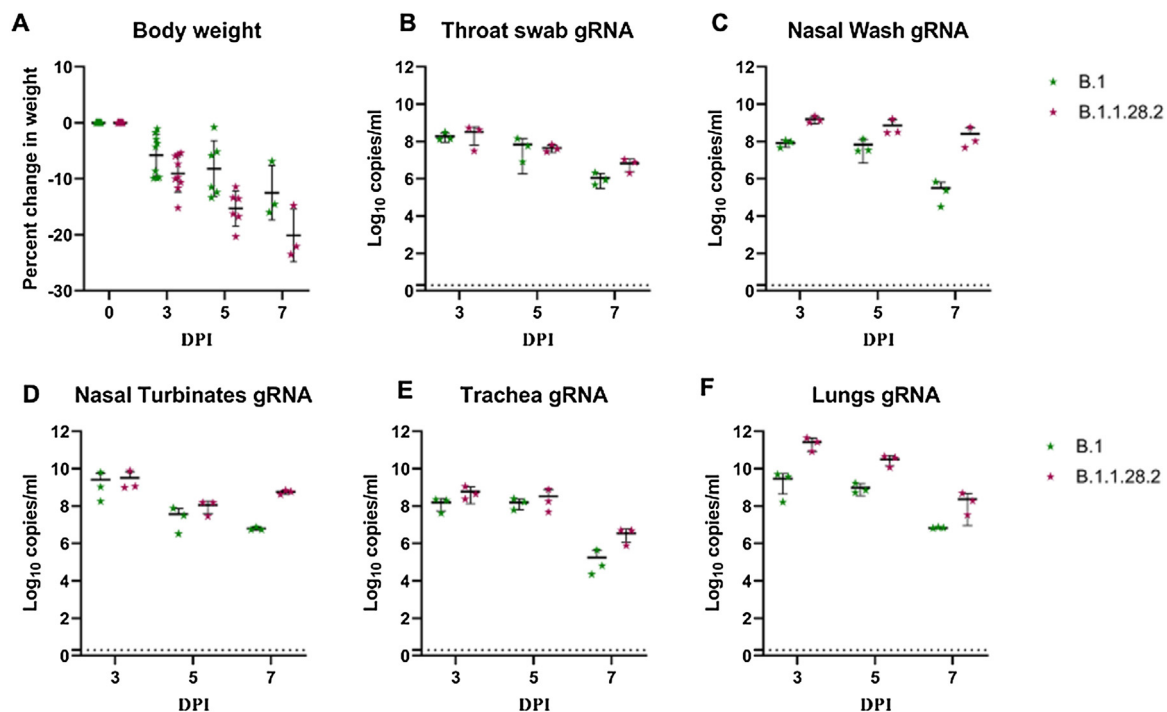
Fig. 2. Body weight change and SARS-CoV-2 viral genomic RNA load in hamsters post inoculation by B.1 and B.1.1.28.2 lineage variants (A) Percent body weight change in hamsters post virus inoculation. Viral load in (B) throat swab (C) nasal wash (D) nasal turbinates (E) trachea and (F) lungs post inoculation.
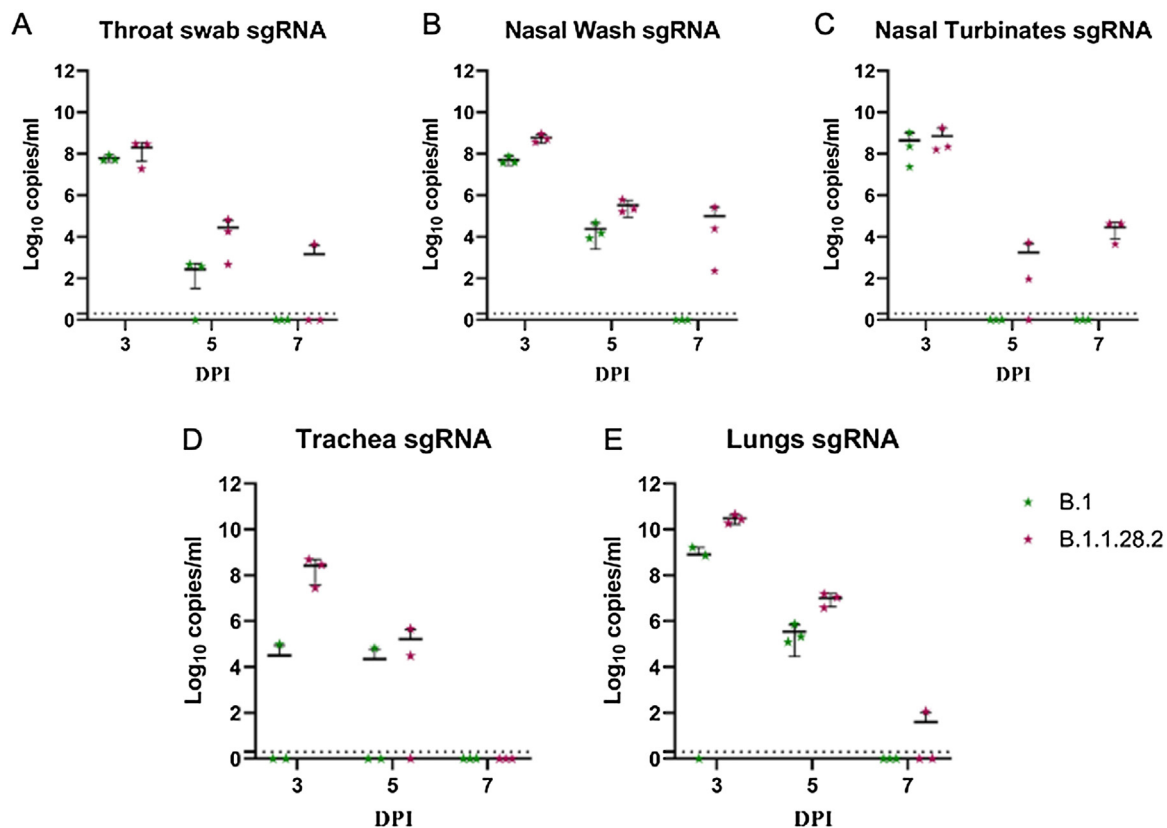

Fig. 3. SARS-CoV-2 viral sub genomic RNA load in hamsters post inoculation by B.1 and B.1.1.28.2 lineage variants. Sub genomic RNA load in (A) throat swab (B) nasal wash (C) nasal turbinates (D) trachea and (E) lungs post inoculation.

Pathogenicity of B.1.1.28.2 in hamsters

We inoculated 9 Syrian hamsters intranasally with 10^4 TCID50 of the B.1.1.28.2 isolate. Body weight loss was observed in ham-sters post inoculation and the average percent weight change in hamsters were -9%, -15% and -20% on day 3, 5 and 7 respec-tively (Fig. 2A). Viral genomic RNA load was highest on day 3
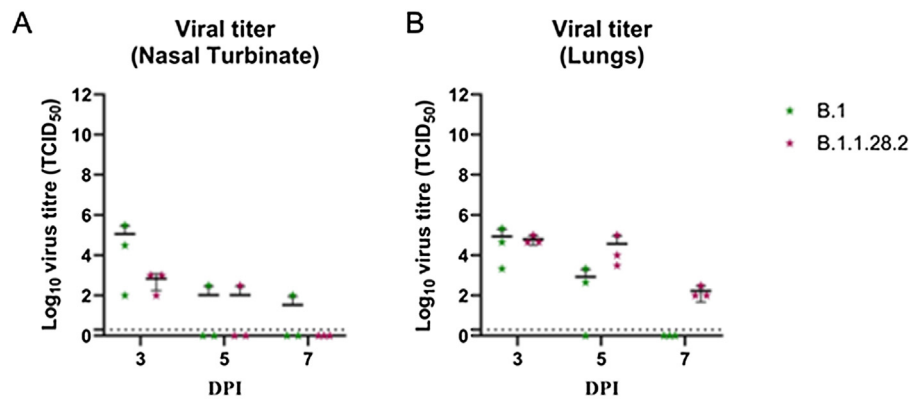
Fig. 4. Viral load by titration. Viral load in (A) nasal turbinates and (B) lungs post infection by SARS-CoV-2.
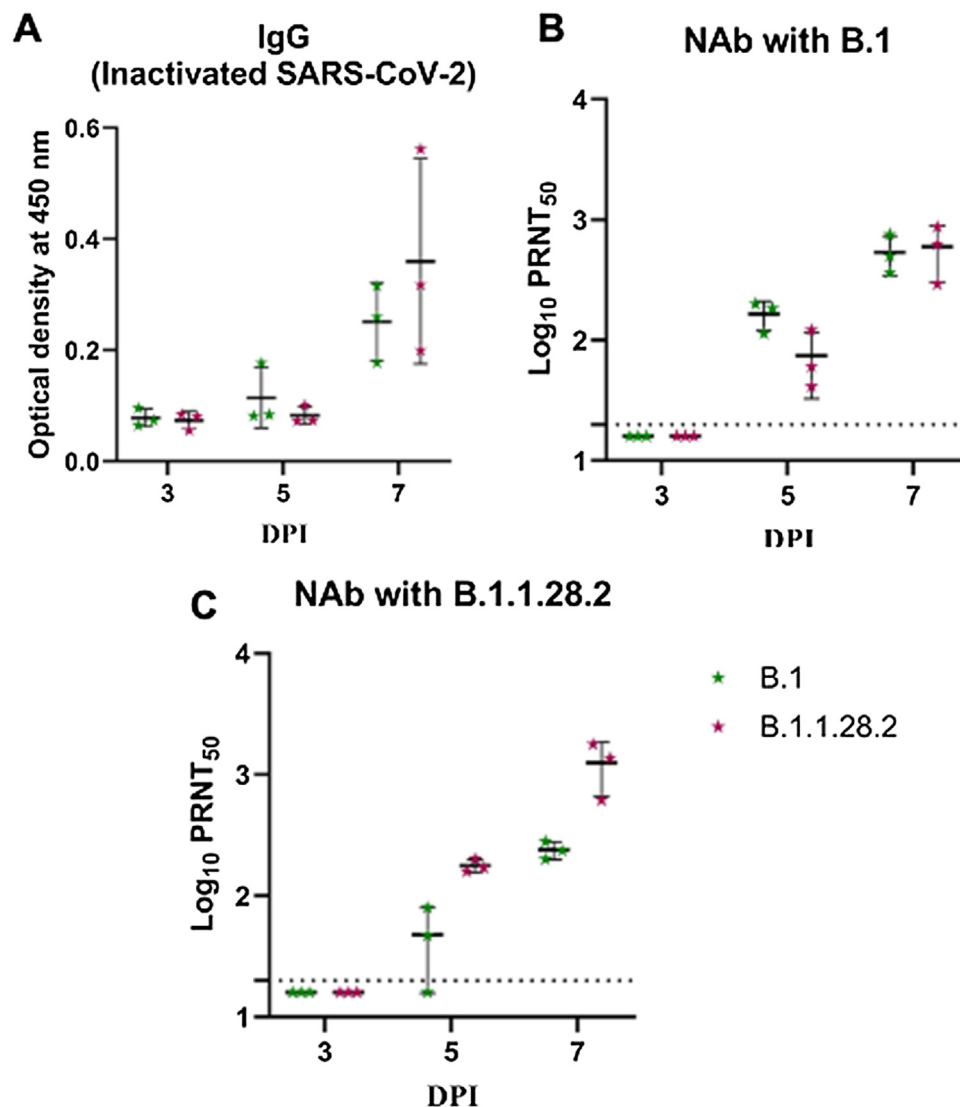

Fig. 5. Comparison of immune response in hamsters post B.1.1.28.2 and B.1 infection. (A) IgG response in hamsters measured by inactivated SARS-CoV-2 IgG ELISA. (B) Neutralizing antibody response in hamsters against B.1 variant (C) Neutralizing antibody response in hamsters against B.1.1.28.2 variant.

and among the organs, lungs (mean = 2.7×10^{11} copies/mL) showed the maximum viral RNA load followed by trachea (mean = 5.9×10^8 copies/mL and nasal turbinate's (mean = 3.2×10^9 copies/ml). Nasal wash and throat swab showed mean gRNA load of 1.6×10^9 and 3.3×10^8 copies/ml (Fig. 2B–F). Viral gRNA load

showed reduction in the further days to reach 2.4×10^8 in lungs, 5.6×10^8 in nasal turbinates and 2.5×10^8 copies/ml in nasal wash.

Sub genomic RNA could be detected in the nasal turbinate and nasal wash samples till day 7 whereas in lungs it could be detected
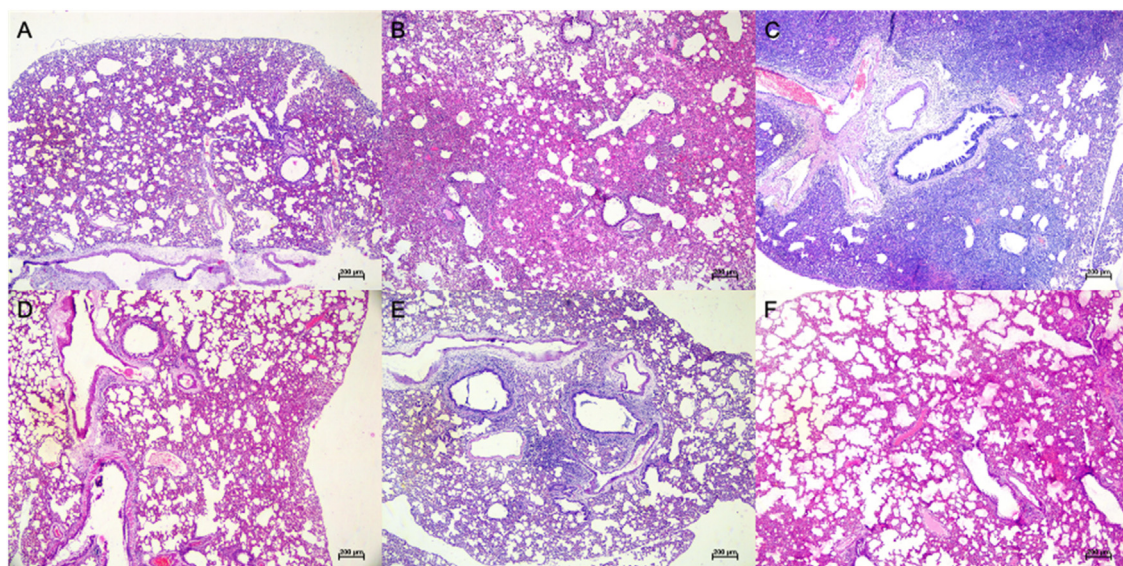
Fig. 6. Histopathological changes in lungs post inoculation by B.1 and B.1.1.28.2 lineage variants. Lungs of hamsters infected with B.1.1.28.2 showing (A) diffuse alveolar capillary congestion and alveolar septal thickening on day 3, (B) diffuse capillary congestion, haemorrhages, consolidation and alveolar septal thickening on day 5 (C) diffuse mononuclear infiltration in the alveolar parenchyma, congested alveolar capillaries and hemorrhages. Lungs of hamsters infected with B.1 variant showing (D) engorged alveolar capillaries and of thickened alveolar septa on day 3 (E) peribronchial mononuclear cell infiltration, alveolar capillary congestion and septal thickening on day 5 (F) an area of consolidation with alveolar hyaline membrane formation, congestion and mononuclear cell infiltration in the alveolar septa on day 7.

till day 5 in all hamsters and in only one hamster on day 7 (Fig. 3). The average virus titer of $10^{4.7}$, $10^{4.16}$ and $10^{2.16}$ TCID50/ml could be observed in lungs on day 3, 5 and 7 respectively, whereas nasal turbinate's showed 100-fold lesser titer than lungs on day 3 and negligible or no titer in the further days (Fig. 4).

Anti-SARS-CoV-2 IgG antibodies could be detected in the serum by day 7 in all hamsters (Fig. 5A). Average neutralization titer of 538.1 and 599.1 were observed in sera of B.1 variant and B.1.1.28.2 variants infected hamsters respectively against B.1 variant. In case of neutralization with B.1.1.28.2 variant an average titer of 240.2 and 1256.3 were observed for B.1 and B.1.1.28.2 variant infected hamsters (Fig. 5B, C). The variant induced severe lung pathological changes in lungs which includes vascular congestion, hemorrhages, interstitial septal thickening with pneumocyte hyperplasia, alveolar consolidation, perivascular, peri-bronchial and interstitial mononuclear cell infiltration. The pneumonic changes were of mild to moderate grade on day 3 which progressed to severe changes on day 7 (Fig. 6A–C, Table 1).

Comparison of pathogenicity of B.1.1.28.2 isolate with B.1 variant in infected hamsters

B.1.1.28.2 lineage variant induced more weight loss in hamsters in comparison to the B.1 variant. The percent weight loss on day 3 (−5%), 5 (−8%) and 7 (−12%) in case of B.1 variant was not statistically significant in comparison to the weight loss observed with B.1.1.28.2 variant (Fig. 2A). Viral genome copies/ml observed in the nasal turbinate's of hamsters infected with B.1 variant was similar to that of the B.1.1.28.2, whereas a hundred-fold lesser average viral gRNA load was observed in the nasal wash (8.3×10^7 copies/ml) on day 3 in case of B.1 variant infected hamsters (Fig. 2C, D). Even though subgenomic RNA were detected in lungs samples on day 3 and 5 for both variants, the B.1 variant infected group showed lesser subgenome copies. On day 7, subgenomic RNA could be detected in 1/3 hamsters infected with B.1.1.28.2 and in none of the hamsters of B.1 infected group (Fig. 3E). Virus titres in lungs of B.1.1.28.2 variant hamsters could be detected till day 7 with an average titre of $10^{4.8}$, $10^{5.05}$ and $10^{2.7}$, on day 3, 5 and 7 respectively. On titration, lungs samples of hamster infected with B.1 variant showed an average

titer of $10^{4.4}$ and $10^{2.95}$ TCID50/ml on day 3 and 5 and no titre on day 7 (Fig. 4B). The pneumonic change observed in lungs induced by B.1 variant was mild in comparison with B.1.1.28.2 (Fig. 6D–F, Table 1).

Discussion

The global spread of emerging SARS-CoV-2 variants, including VOCs has heightened concerns about enhanced transmissibility, virulence, and attenuation of susceptibility to humoral immunity elicited by natural infection or vaccination. Lack of clinical data and transmissibility studies of the B.1.1.28 P.1 and P.2 variants, make the course of infection in affected individual unpredictable. Here we isolated P2 variant from international travelers returned to India and characterized the isolate. The characteristic spike mutations in P2 lineage are D614G, E484K and V1176F. These mutations were reported in many VOCs and VOIs which are rapidly spreading worldwide and E484K substitution is known for immune evasion potential [19].

We observed disease in hamster model characterized by the weight loss and lung pneumonic changes similar to other SARS-CoV-2 variants. COVID-19 in hamsters is characterized by respiratory signs, body weight loss and pneumonia [20]. Hamster model has been used to assess the infectivity and pathogenicity of SARS-CoV-2 VOCs like B.1.1.7, B.1.351, B.1.617 etc [17,21]. The variant specific differences can be evaluated with this model using criteria's like viral load, histological scoring, inflammatory cytokine level etc [17,21]. B.1.1.28.2 variant induced body weight loss and supported viral replication in respiratory tract. Here, live infectious virus could be detected till day 7 in lung samples whereas in nasal turbinates it was detected only on day 3 and with 100-fold lesser titer indicating the virus predilection to the lower respiratory tract. Viral gRNA shed through nasal wash was higher in case of B.1.1.28.2. High viral shedding through nasal wash could be linked to the increased transmission efficiency speculated for this variant. For this further transmission studies needs to be performed.

In comparison with B.1 variant, the pathogenicity of the isolate was more with severe pneumonia. Although, variants of concern

Table 1

Average cumulative histopathological score of the lung lesions (vascular changes, alveolar damage and inflammatory changes) in hamsters infected with B.1 and B.1.1.28.2 lineage variant.

Days post infection	B.1 lineage variant			B.1.1.28.2 lineage variant		
	Animal 1	Animal 2	Animal 3	Animal 1	Animal 2	Animal 3
3	+1	+1	+1	+3	+2	+3
5	+2	+2	+1	+3	+3	+3
7	+2	+2	+1	+3	+4	+4

are speculated to be linked to increased disease severity and transmission, in vivo experimental studies in case of B.1.1.7 and B.1.351 showed less or comparable disease severity with earlier SARS-CoV-2 strains [17,21]. B.1.1.7 variant showed comparable lung pathology in hamster model in comparison to B.1 [17]. Also B.1.1.7 and B.1.351 studies in hamster and non-human primate models did not show any increased disease severity [17,21,22]. In contrary, here we observed severe pneumonic changes associated with a variant of interest i.e., Brazil P2 variant.

Since the mutation in the E484 site in the RBD known to have the large effect on binding and neutralization of the SARS-CoV-2 is present in the B.1.1.28.2 variant, we assessed the neutralization potential of the hamster sera. Comparable neutralization efficiency was shown by both B.1 and B.1.1.28.2 variants infected hamster sera against B.1 variant, whereas reduction was seen in the neutralization titre of B.1 infected hamster sera against B.1.1.28.2. This finding is in line with the earlier reports of neutralization reduction in case of monoclonal antibody treatment and post vaccination sera by P.2 variant [8,23]. Reinfection cases have also been reported with E484K mutation [19]. The neutralization efficacy of B.1.1.28.2 variant was assessed with the convalescent sera of COVID-19 infected individual sera and BBV152 two-dose vaccinated individuals to observe about two-fold reductions in neutralizing titer against B.1.1.28.2 variant [24].

Conclusions

Here we report the isolation and characterization of the B.1.1.28.2 variant from international travelers returned to India and its characterization. The isolate was found pathogenic in hamsters producing severe pneumonia in comparison with B.1 lineage variant infection. Neutralization reduction against B.1.1.28.2 was observed in case of B.1 lineage variant infection indicating need for screening vaccines for efficacy against the variant.

Data availability

All the data is included in the manuscript and the GISAID identifiers have been provided for the SARS-CoV-2 isolates.

Author contributions

PDY and SM contributed to study design and paper writing, PDY, NG and VP contributed to patient data collection, genomic data analysis and interpretation. SM performed animal experiments and experimental data collection. PDY, AS, DAN contributed to data analysis and interpretation, writing and critical review. RRS contributed to patient data collection, writing and critical review. GS, PS and SB contributed to laboratory investigations. PA, SP and BB contributed to writing and critical review of the manuscript.

Funding

Declaration of interests

No conflict of interest exists among authors.

Acknowledgements

References

[1] World Health Organization. COVID-19 Weekly Epidemiological Update, Edition 60, published 5 October 2021. https://www.who.int/publications/m/item/weekly-epidemiological-update-on-covid-19—5-october-2021. [Accessed 11 October 2021].

[2] Tegally H, Wilkinson E, Giovanetti M, Iranzadeh A, Fonseca V, Giandhari J, et al. Emergence and rapid spread of a new severe acute respiratory syndrome-related coronavirus 2 (SARS267 CoV-2) lineage with multiple spike mutations in South Africa. medRxiv 2020, http://dx.doi.org/10.1101/2020.12.21.20248640.

[3] Faria NR, Mellan TA, Whittaker C, Claro IM, Candido DDS, Mishra S, et al. Genomics and epidemiology of the P.1 SARS-CoV-2 lineage in Manaus, Brazil. Science 2021:eabh2644.

[4] Centers for Disease Control and Prevention (CDC). Emerging SARS-CoV-2 Variants. https://www.cdc.gov/coronavirus/2019-ncov/science/science-briefs/scientific-brief-emerging-variants.html. [Accessed 12 February 2021].

[5] Cherian S, Potdar V, Jadhav S, Yadav P, Gupta N, Das M, et al. SARS-CoV-2 Spike Mutations, L452R, T478K, E484Q and P681R, in the Second Wave of COVID-19 in Maharashtra, India. Microorganisms 2021;9(7):1542, http://dx.doi.org/10.3390/microorganisms9071542.

[6] Farasani A. Biochemical role of serum ferratin and d-dimer parameters in COVID 19 diagnosis. Saudi J Biol Sci 2021;28(12):7486–90, http://dx.doi.org/10.1016/j.sjbs.2021.08.040.

[7] Yadav P, Sapkal GN, Abraham P, Ella R, Deshpande G, Patil DY, et al. Neutralization of variant under investigation B. 1.617 with sera of BBV152 vaccinees. Clin Infect Dis 2021:ciab411, http://dx.doi.org/10.1093/cid/ciab411.

[8] Garcia-Beltran WF, Lam EC, Denis KS, Nitido AD, Garcia ZH, Hauser BM, et al. Multiple SARS-CoV-2 variants escape neutralization by vaccine-induced humoral immunity. Cell 2021;184(9):2372–83, http://dx.doi.org/10.1016/j.cell.2021.03.013.

[9] Muñoz-Fontela C, Dowling WE, Funnell SG, Gsell PS, Riveros-Balta AX, Albrecht RA, et al. Animal models for COVID-19. Nature 2020;586(7830):509–15, http://dx.doi.org/10.1038/s41586-020-2787-6.

[10] Mohandas S, Yadav PD, Nyayanit D, Deshpande G, Aich A, Sapkal G, et al. Comparison of the pathogenicity and virus shedding of SARS CoV-2 VOC 202012/01 and D614G variant in hamster model. bioRxiv 2021, http://dx.doi.org/10.1101/2021.02.25.432136.

[11] Yadav PD, Mohandas S, Shete AM, Nyayanit DA, Gupta N, Patil DY, et al. SARS CoV-2 variant B.1.617.1 is highly pathogenic in hamsters than B.1 variant. bioRxiv 2021, http://dx.doi.org/10.1101/2021.05.05.442760.

[12] Reed LJ, Muench H. A simple method of estimating fifty per cent endpoints. Am J Epidemiol 1938;27(3):493–7.

[13] Sarkale P, Patil S, Yadav PD, Nyayanit DA, Sapkal G, Baradkar S, et al. First isolation of SARS-CoV-2 from clinical samples in India. Indian J Med Res 2020;151(2–3):244, http://dx.doi.org/10.4103/ijmr.IJMR_1029_20.

[14] Yadav PD, Nyayanit DA, Shete AM, Jain S, Majumdar TP, Chaubal GY, et al. Complete genome sequencing of Kaisodi virus isolated from ticks in India belonging to Phlebovirus genus, family Phenuiviridae. Ticks Tick Borne Dis 2019;10(1):23–33.

[15] Choudhary ML, Vipat V, Jadhav S, Basu A, Cherian S, Abraham P, et al. Development of in vitro transcribed RNA as positive control for laboratory diagnosis of SARS-CoV-2 in India. Indian J Med Res 2021;151(2):251, http://dx.doi.org/10.4103/ijmr.IJMR_671_20.

[16] Wölfel R, Corman VM, Guggemos W, Seilmaier M, Zange S, Muller MA, et al. Virological assessment of hospitalized patients with COVID-2019. Nature 2020;581(7809):465–9, http://dx.doi.org/10.1038/s41586-020-2196-x.

[17] Mohandas S, Yadav PD, Shete-Aich A, Abraham P, Vadrevu KM, Sapkal G, et al. Immunogenicity and protective efficacy of BBV152, whole virion inactivated SARS-CoV-2 vaccine candidates in the Syrian hamster model. Iscience 2021;24(2):102054.

[18] Deshpande GR, Sapkal GN, Tilekar BN, Yadav PD, Gurav Y, Gaikwad S, et al. Neutralizing antibody responses to SARS-CoV-2 in COVID-19 patients. Indian J Med Res 2020;152(1):82–7.

[19] Nonaka CK, Franco MM, Gräf T, de Lorenzo Barcia CA, de Ávila Mendonça RN, De Sousa KA, et al. Genomic evidence of SARS-CoV-2 reinfection involving E484K spike mutation, Brazil. Emerg Infect Dis 2021;27(5):1522.

[20] Mohandas S, Jain R, Yadav PD, Shete-Aich A, Sarkale P, Kadam M, et al. Evaluation of the susceptibility of mice & hamsters to SARS-CoV-2 infection. Indian J Med Res 2020;151(5):479, http://dx.doi.org/10.4103/ijmr.IJMR_2235_20.

[21] Abdelnabi R, Boudewijns R, Foo CSY, Seldeslachts L, Sanchez-Felipe L, Zhang X, et al. Comparative infectivity and pathogenesis of emerging SARS-CoV-2 variants in Syrian hamsters. EBioMedicine 2021;68:103403, http://dx.doi.org/10.1016/j.ebiom.2021.103403.

[22] Munster V, Flagg M, Singh M, Williamson B, Feldmann F, Perez-Perez L, et al. Subtle differences in the pathogenicity of SARS-CoV-2 variants of concern B.1.1.7 and B.1.351 in rhesus macaques. Sci Adv 2021;7(43):eabj3627, http://dx.doi.org/10.1126/sciadv.abj3627.

[23] Centers for Disease Control and Prevention. SARS-CoV-2 variant classifications and definitions. https://www.cdc.gov/coronavirus/2019-ncov/cases-updates/variant-surveillance/variant-info.html. [Accessed 16 March 2021].

[24] Sapkal G, Yadav PD, Ella R, Abraham P, Patil DY, Gupta N, et al. Neutralization of B.1.1.28 P2 variant with sera of natural SARS-CoV-2 infection and recipients of BBV152 vaccine. J Travel Med 2021;28(7):taab077, http://dx.doi.org/10.1093/jtm/taab077.